

## Article

# Synthesis of $\theta$ - $\text{Al}_2\text{O}_3$ Whiskers with Twins

Nan Liao <sup>1,2</sup>, Xiaojia Su <sup>1</sup>, Haiwen Zhang <sup>1</sup>, Qingguo Feng <sup>1</sup>, Salvatore Grasso <sup>1</sup>  and Chunfeng Hu <sup>1,\*</sup> 

<sup>1</sup> Key Laboratory of Advanced Technologies of Materials, Ministry of Education, School of Materials Science and Engineering, Southwest Jiaotong University, Chengdu 610031, China; 18782151072@163.com (N.L.); suxiaojia1993@163.com (X.S.); 18326218394@163.com (H.Z.); qfeng@swjtu.edu.cn (Q.F.); s.grasso@swjtu.edu.cn (S.G.)

<sup>2</sup> Science and Technology on Reactor System Design Technology Laboratory, Nuclear Power Institute of China, Chengdu 610213, China

\* Correspondence: chfhu@live.cn; Tel.: +86-150-0284-9860

**Abstract:** In this work,  $\theta$ - $\text{Al}_2\text{O}_3$  whiskers with twins were successfully fabricated by a hydrothermal method followed by annealing at 1000 °C in argon atmosphere using  $\text{Al}_2(\text{SO}_4)_3 \cdot 18\text{H}_2\text{O}$ ,  $\text{CO}(\text{NH}_2)_2$  and PEG2000 as initial materials. It is confirmed that precursor of  $\text{AlO}(\text{OH})$  whiskers is suitable to be used for preparing alumina whiskers when the molar ratio of  $\text{Al}^{3+}:\text{CO}(\text{NH}_2)_2$  is selected to be 1:6. The mean length of obtained whiskers is 1.5  $\mu\text{m}$  and the average width is 0.1  $\mu\text{m}$ . Interestingly, it is found that the as-prepared  $\theta$ - $\text{Al}_2\text{O}_3$  whiskers consist of twins with (100) plane as the twin surface, which is ascribed to the phase transformation from tetragonal phase ( $\delta$ - $\text{Al}_2\text{O}_3$ ) to monoclinic phase ( $\theta$ - $\text{Al}_2\text{O}_3$ ) during the annealing. Additionally, the specific surface area of  $\theta$ - $\text{Al}_2\text{O}_3$  whiskers is measured to be 38.2  $\text{m}^2/\text{g}$ .

**Keywords:**  $\theta$ - $\text{Al}_2\text{O}_3$  whisker; synthesis; microstructure; specific surface area



**Citation:** Liao, N.; Su, X.; Zhang, H.; Feng, Q.; Grasso, S.; Hu, C. Synthesis of  $\theta$ - $\text{Al}_2\text{O}_3$  Whiskers with Twins. *Metals* **2021**, *11*, 895. <https://doi.org/10.3390/met11060895>

Academic Editor: Frank Czerwinski

Received: 8 May 2021

Accepted: 28 May 2021

Published: 30 May 2021

**Publisher's Note:** MDPI stays neutral with regard to jurisdictional claims in published maps and institutional affiliations.



**Copyright:** © 2021 by the authors. Licensee MDPI, Basel, Switzerland. This article is an open access article distributed under the terms and conditions of the Creative Commons Attribution (CC BY) license (<https://creativecommons.org/licenses/by/4.0/>).

## 1. Introduction

Owing to the high strength, high modulus, high hardness and excellent corrosion resistance against acid and alkaline, ceramic whiskers with tiny defects have been widely investigated in the last twenty years [1–4]. To date, it is known that mullite whisker, TiCN whisker and SiC whisker etc. have been successfully synthesized and potentially used as the reinforcing and toughening phases in the ceramic-based composites, diesel particulate filters, catalytic supporters and drug delivers [5–14]. For example, Z. Zhao et al. fabricated 15 vol.%  $\text{TiC}_{0.3}\text{N}_{0.7}$  whisker reinforced  $\beta$ -sialon composite at 1750 °C under 30 MPa and confirmed that the hardness and fracture toughness were effectively improved [11]. Similarly, Y. Luo et al. designed SiC-SiO<sub>2</sub>-Al<sub>2</sub>O<sub>3</sub> triple-layered SiC whisker to toughen SiC composite and determined that the high flexural strength of 533.3 MPa and high fracture toughness of 13.6 MPa  $\text{m}^{1/2}$  could be achieved [13]. In addition, by using the loose stacking capability of whisker, porous ceramic could be well prepared. Y.M. Zhang et al. have prepared mullite frameworks using vapor-solid reaction with SiO<sub>2</sub>, Al<sub>2</sub>O<sub>3</sub> and AlF<sub>3</sub> as the forming agent at 1500 °C and determined that the framework possessed high porosity of 62.3% and high compressive strength of 142 MPa [14].

For Al<sub>2</sub>O<sub>3</sub> whiskers, to date, there are mainly two methods to prepare: one is the high temperature growth by vapor-liquid-solid deposition (VLS) and another is the hydrothermal reaction followed by high temperature annealing. The second method is more convenient and not very critical to produce a large amount of whiskers. About the application of Al<sub>2</sub>O<sub>3</sub> whiskers, X.Y. Qu et al. have fabricated  $\gamma$ -Al<sub>2</sub>O<sub>3</sub> whisker reinforced aluminum composite by in situ cold pressing and sintering and confirmed that the tensile strength and hardness of composite could be greatly upgraded [15]. In addition, Y. Tamura et al. found that by using  $\alpha$ -Al<sub>2</sub>O<sub>3</sub> whisker to reinforce Al<sub>2</sub>O<sub>3</sub> ceramic through spark plasma sintering the high temperature creep resistance of composite was improved up to one order of magnitude in comparison with that of pure Al<sub>2</sub>O<sub>3</sub> specimen [16]. In

addition, M. Ali et al. fabricated the PEGylated porous  $\alpha$ -Al<sub>2</sub>O<sub>3</sub> whiskers and found that it had excellent biocompatibility and drug loading and release characteristic [17], whereas, until now, no research has been done to investigate  $\theta$ -Al<sub>2</sub>O<sub>3</sub> whisker. Since it is also one high temperature phase member of alumina whiskers, it is believed that except the members of  $\gamma$ -Al<sub>2</sub>O<sub>3</sub> and  $\alpha$ -Al<sub>2</sub>O<sub>3</sub> whiskers [18–25] the  $\theta$ -Al<sub>2</sub>O<sub>3</sub> whisker may also play one important reinforcing role in the composites.

In this paper,  $\theta$ -Al<sub>2</sub>O<sub>3</sub> whiskers were successfully prepared by the hydrothermal method followed by high temperature annealing. The optimized molar ratio of initial materials to synthesize  $\theta$ -Al<sub>2</sub>O<sub>3</sub> whiskers was confirmed and the microstructure and adsorption property of whiskers were characterized.

## 2. Experimental Procedure

Commercial powders of Al<sub>2</sub>(SO<sub>4</sub>)<sub>3</sub>·18H<sub>2</sub>O (99.5%), CO(NH<sub>2</sub>)<sub>2</sub> (99.5%) and PEG2000 (99.5%) were used to fabricate the precursors [26]. In order to control the microstructure of precursors, the molar ratios of Al<sup>3+</sup>:CO(NH<sub>2</sub>)<sub>2</sub> were designed as 1:3, 1:5, 1:6 and 1:7. The weighed powders were put into a hydrothermal kettle and then mixed with the deionized water and ultrasonically stirred for 30 min until all powders dissolved into the solution. Then, the kettle containing solution was sealed and put in an oven and heated at 150 °C for 12 h. After removing the deposited powder by vacuum filtration, the obtained precursor was dried in the oven. The composition of precursor was examined by a X-ray diffractometer (XRD) facility (Bruker D8 ADVANCE A25X, Bruker Corporation Co. Ltd., Karlsruhe, Germany) operated at 40 kV and 40 mA. The morphology of precursors was observed by a scanning electron microscope (SEM) (FEI Inspect F50, Hillsboro, OR, USA) equipped with an energy dispersive spectrometer (EDS) (Oxford Instruments, Oxford, UK).

In order to obtain the  $\theta$ -Al<sub>2</sub>O<sub>3</sub> whiskers, the prepared precursors were put into an alumina crucible and annealed at 1000 °C in a tube furnace in flowing argon atmosphere. The heating speed was 10 °C/min and the holding time was 6 h. Then, the compositions of powders were examined by XRD and the microstructure of whiskers was observed by SEM. The atomic arrangement of as-prepared  $\theta$ -Al<sub>2</sub>O<sub>3</sub> whiskers was checked by a transmission electron microscope (TEM) (ZEISS Libra 200 FE, CARL ZEISS Co. Ltd., Baden Wuerttemberg, Germany). The whiskers were dispersed in ethanol by ultrasonically stirring for 10 min and then the suspension was dropped onto a copper web. Additionally, the specific surface area of  $\theta$ -Al<sub>2</sub>O<sub>3</sub> whiskers was measured by a BET apparatus (*QuadraSorb Station 1*, Quantachrome Instruments, Boynton Beach, FL, USA) with liquid nitrogen adsorption at −196 °C after degassing at 300 °C for 6 h.

## 3. Results and Discussion

Figure 1 shows the X-ray diffraction (XRD) patterns of dried precursors prepared by hydrothermal method, presenting the effect of urea content on the composition of deposited precursors. It is seen that with the decreased molar ratio of Al<sup>3+</sup>:CO(NH<sub>2</sub>)<sub>2</sub> the phase compositions of obtained powders change correspondingly. When the molar ratio is 1:3, the obtained precursor probably consists of AlO(OH) and NH<sub>4</sub>Al<sub>3</sub>(SO<sub>4</sub>)<sub>2</sub>(OH)<sub>6</sub> in which NH<sub>4</sub>Al<sub>3</sub>(SO<sub>4</sub>)<sub>2</sub>(OH)<sub>6</sub> is the main phase (Figure 1a). When the molar ratios are decreased to 1:5 and 1:6, the determined phase is AlO(OH) without any other impurities (Figure 1b,c). By continuously decreasing the molar ratio of Al<sup>3+</sup>:CO(NH<sub>2</sub>)<sub>2</sub> to be 1:7, the main phase is NH<sub>4</sub>Al(OH)<sub>2</sub>CO<sub>3</sub> and a few AlO(OH) phase coexists (Figure 1d). Based on the analysis of XRD results, it is concluded that the preferentially formed phases are NH<sub>4</sub>Al<sub>3</sub>(SO<sub>4</sub>)<sub>2</sub>(OH)<sub>6</sub>, AlO(OH) and NH<sub>4</sub>Al(OH)<sub>2</sub>CO<sub>3</sub> respectively with the increasing content of urea. The reason might be that with the increasing content of urea the pH value of solution increases owing to the existence of more OH<sup>−</sup> and CO<sub>3</sub><sup>2−</sup> ions released by more urea in the solution so as to result in the formation of precursors with weaker acidity [12].

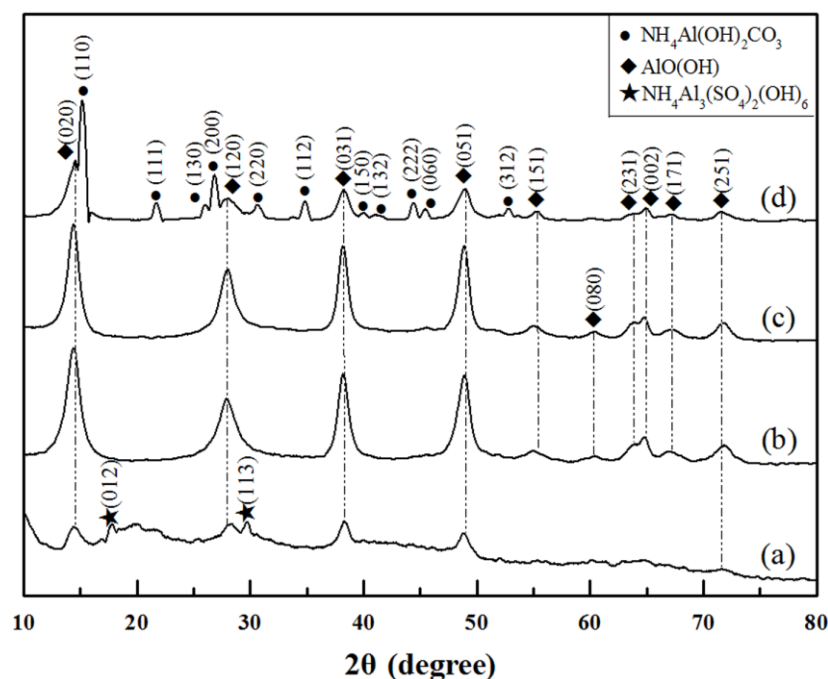


**Figure 1.** X-ray diffraction (XRD) patterns of deposited precursors fabricated by hydrothermal method under different molar ratio of  $\text{Al}^{3+}:\text{CO}(\text{NH}_2)_2$ : (a) 1:3, (b) 1:5, (c) 1:6 and (d) 1:7.

In order to clearly understand the morphology change of whiskers with different urea content, scanning electron microscope (SEM) was adopted to observe the deposited powders, as shown in Figure 2. It is seen that when the molar ratio of  $\text{Al}^{3+}:\text{CO}(\text{NH}_2)_2$  is selected as 1:3, most of obtained precursors are balls covered by oriented whiskers (Figure 2a). The mean size of balls is measured as 7.8  $\mu\text{m}$ . By increasing the content of urea, all balls disappear when the molar ratios of  $\text{Al}^{3+}:\text{CO}(\text{NH}_2)_2$  are 1:5 and 1:6 and all formed precursors are agglomerated oriented whiskers like chrysanthemum (Figure 2b,c). The length of both whiskers is about 1.5  $\mu\text{m}$  and the mean widths of whiskers are 0.1 and 0.15  $\mu\text{m}$  respectively. Based on the XRD spectra in Figure 1, it is concluded that the balls are  $\text{NH}_4\text{Al}_3(\text{SO}_4)_2(\text{OH})_6$  phase and the whiskers are  $\text{AlO}(\text{OH})$  phase. Under the higher urea loading with the molar ratio of  $\text{Al}^{3+}:\text{CO}(\text{NH}_2)_2$  of 1:7, most of the whiskers disperse like beams (Figure 2d). This result can be explained by the Von Weimarn's theory that when increasing the concentration of urea the energy for formation of new surfaces is available [12,27]. It is confirmed that the new formed whiskers are  $\text{NH}_4\text{Al}(\text{OH})_2\text{CO}_3$  phase and with the increasing content of urea the morphology of deposited precursors exhibits the tendency of ball to flower to beam corresponding to the phase transformation of  $\text{NH}_4\text{Al}_3(\text{SO}_4)_2(\text{OH})_6$  to  $\text{AlO}(\text{OH})$  to  $\text{NH}_4\text{Al}(\text{OH})_2\text{CO}_3$ .

Additionally, in order to fabricate  $\theta\text{-Al}_2\text{O}_3$  whiskers, the as-prepared precursors were annealed at 1000  $^\circ\text{C}$  for 6 h. M. Digne et al. confirmed that the precursor of  $\text{AlO}(\text{OH})$  could be transformed into  $\gamma\text{-Al}_2\text{O}_3$  at 450  $^\circ\text{C}$ ,  $\delta\text{-Al}_2\text{O}_3$  at 750  $^\circ\text{C}$  and  $\theta\text{-Al}_2\text{O}_3$  at 1000  $^\circ\text{C}$  [28]. Figure 3 shows the XRD spectra of annealed powders under the different urea loading. It is found that when the molar ratio of  $\text{Al}^{3+}:\text{CO}(\text{NH}_2)_2$  is 1:3 the diffraction peaks belong to  $\gamma\text{-Al}_2\text{O}_3$  (Figure 3a). It is a very interesting phenomenon to form  $\gamma\text{-Al}_2\text{O}_3$  phase at a high temperature of 1000  $^\circ\text{C}$ , which supplies one possible way to prepare high temperature  $\gamma\text{-Al}_2\text{O}_3$  phase transformed from  $\text{NH}_4\text{Al}_3(\text{SO}_4)_2(\text{OH})_6$ . When the molar ratios of  $\text{Al}^{3+}:\text{CO}(\text{NH}_2)_2$  are 1:5, 1:6 and 1:7, though the precursors of  $\text{AlO}(\text{OH})$  and  $\text{NH}_4\text{Al}(\text{OH})_2\text{CO}_3$  are different, the final products are same to be  $\theta\text{-Al}_2\text{O}_3$  phase and crystallize very well (Figure 3b–d). It is determined that the sintering temperature of 1000  $^\circ\text{C}$  and holding time of 6 h are suitable for fabricating high purity  $\theta\text{-Al}_2\text{O}_3$  whiskers. K. Morinaga et al. also found that at the temperature range of 950–1150  $^\circ\text{C}$  the  $\theta\text{-Al}_2\text{O}_3$  could be existing stably [24].

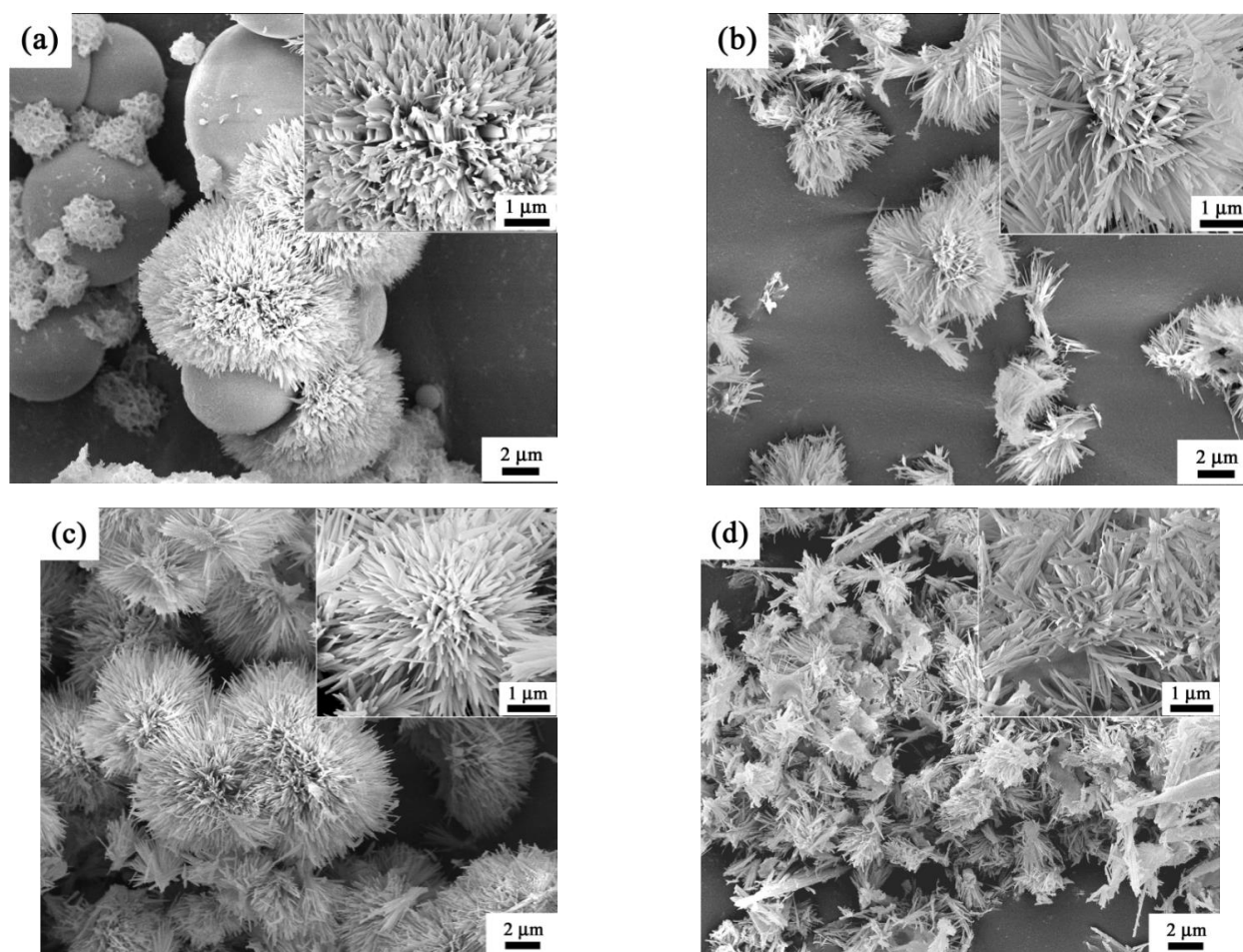


**Figure 2.** Scanning electron microscope (SEM) images of deposited precursors prepared by the hydrothermal method with different molar ratio of  $\text{Al}^{3+}:\text{CO}(\text{NH}_2)_2$ : (a) 1:3, (b) 1:5, (c) 1:6 and (d) 1:7.

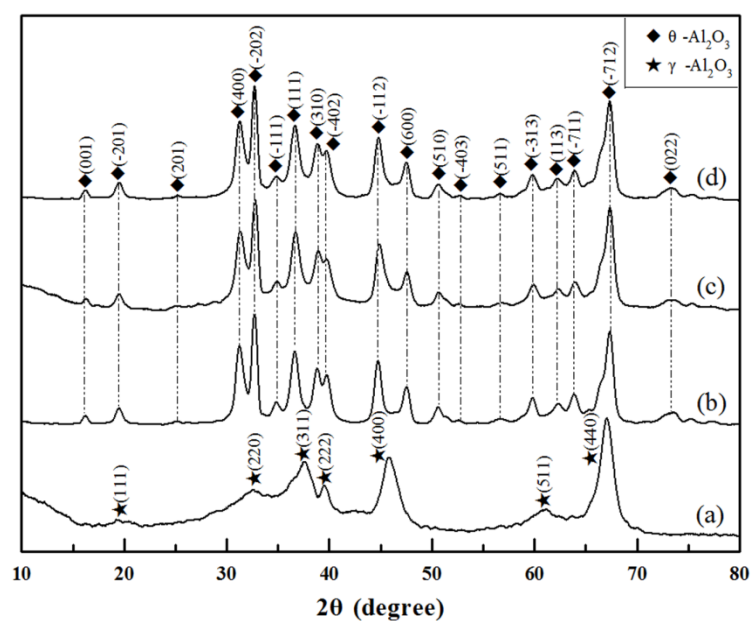


**Figure 3.** XRD spectra of annealed powders treated at 1000 °C for 6 h using the precursors prepared by the hydrothermal method with the different molar ratio of  $\text{Al}^{3+}:\text{CO}(\text{NH}_2)_2$ : (a) 1:3, (b) 1:5, (c) 1:6 and (d) 1:7. The referred diffraction peaks of  $\gamma\text{-Al}_2\text{O}_3$  are from ICSD 66559.



Furthermore, by observing the microstructure of annealed powders using SEM, it is seen that the morphology of powders does not change much in comparison with the precursors, as shown in Figure 4. At the molar ratio of  $\text{Al}^{3+}:\text{CO}(\text{NH}_2)_2$  of 1:3, the formed  $\gamma\text{-Al}_2\text{O}_3$  phase shows the ball-like structure (Figure 4a). With the increasing content of urea relative to the molar ratios of  $\text{Al}^{3+}:\text{CO}(\text{NH}_2)_2$  of 1:5 and 1:6, the obtained  $\theta\text{-Al}_2\text{O}_3$  phase presents the chrysanthemum-like microstructure (Figure 4b,c). Especially, at the molar ratio of  $\text{Al}^{3+}:\text{CO}(\text{NH}_2)_2$  of 1:6, the prepared chrysanthemum-like whiskers are more homogeneous. Additionally, when the molar ratio of  $\text{Al}^{3+}:\text{CO}(\text{NH}_2)_2$  is 1:7, only beam-like  $\theta\text{-Al}_2\text{O}_3$  whiskers could be examined (Figure 4d). It is known that the formation of whiskers is ascribed to the decomposition of precursors by giving off ammonia and carbon dioxide and the recrystallization by phase transformation [29]. It exhibits that the final morphology of  $\theta\text{-Al}_2\text{O}_3$  whiskers is dependent on the initial morphology of precursors. Therefore, the optimized molar ratio of  $\text{Al}^{3+}:\text{CO}(\text{NH}_2)_2$  of 1:6 is suitable for the preparation of  $\theta\text{-Al}_2\text{O}_3$  whiskers.

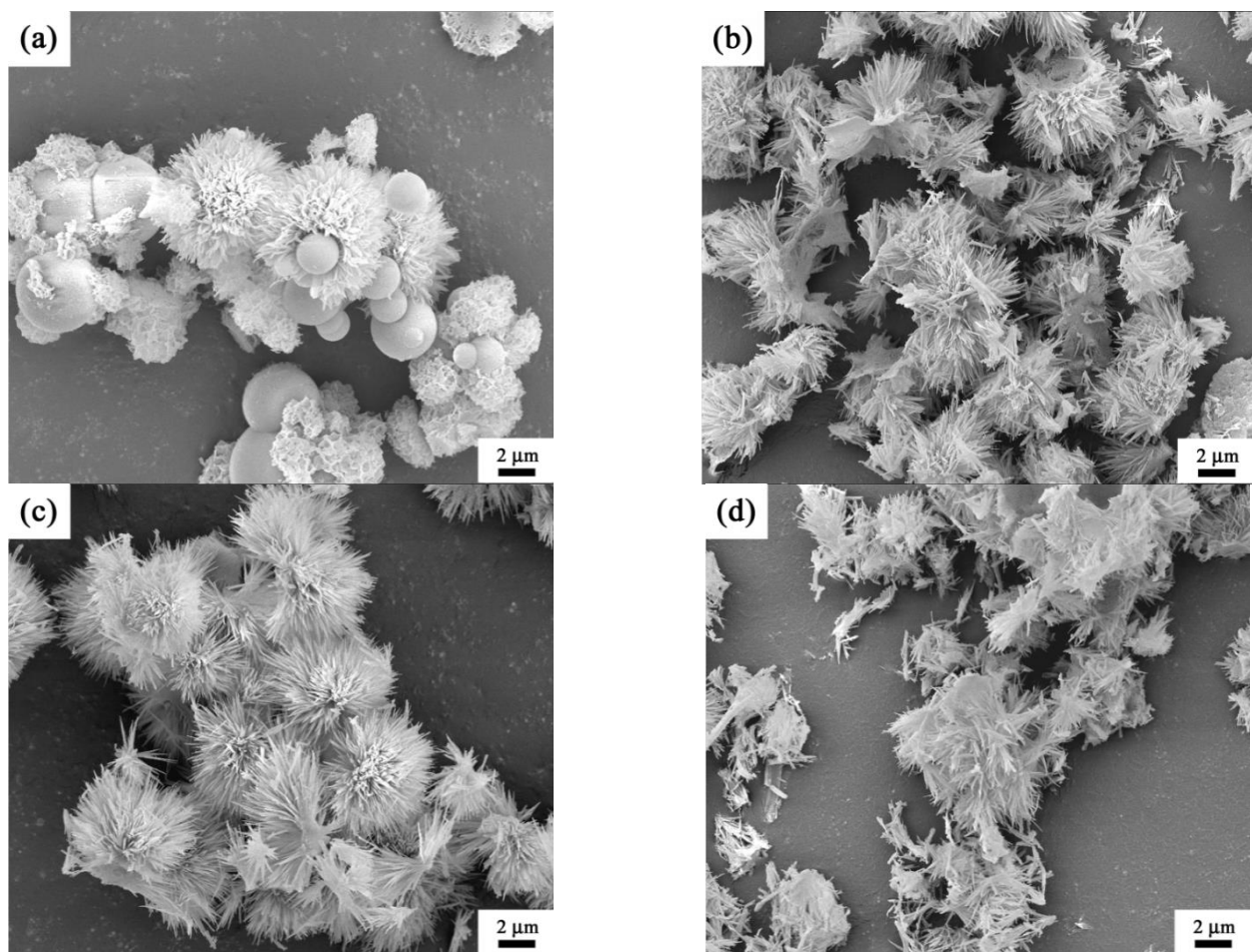


**Figure 4.** SEM micrographs of annealed powders transformed from the precursors prepared by the hydrothermal method under the different molar ratio of  $\text{Al}^{3+}:\text{CO}(\text{NH}_2)_2$ : (a) 1:3, (b) 1:5, (c) 1:6 and (d) 1:7.

To characterize the  $\theta\text{-Al}_2\text{O}_3$  whiskers in details, the transmission electron microscope (TEM) was utilized to observe the microstructure of annealed powder transformed from the  $\text{AlO}(\text{OH})$  precursor prepared with the molar ratio of  $\text{Al}^{3+}:\text{CO}(\text{NH}_2)_2$  of 1:6. Figure 5 shows the highly magnified image and atomic arrangement of  $\theta\text{-Al}_2\text{O}_3$  whiskers, as well as the selected area electron diffraction (SAED) pattern. It is seen that the tips of whiskers are smooth (Figure 5a). Interestingly, it is found that the obtained whiskers are monoclinic with twins. The twin surface is (100) plane and (102) plane is deflected for a certain angle (Figure 5b). In addition, the double SAED pattern confirms the existence of

twins. The formation of twinned  $\theta$ - $\text{Al}_2\text{O}_3$  whiskers is probably associated with the phase transformation from tetragonal system ( $\delta$ - $\text{Al}_2\text{O}_3$ ) to monoclinic system ( $\theta$ - $\text{Al}_2\text{O}_3$ ) [30–33]. Y.G. Wang et al. also found in the  $\theta$ - $\text{Al}_2\text{O}_3$  powder there existed multiple twinned lamellae arranged along the [001] direction, which was possibly owing to the frozen-in stages during the phase transition [32]. Present phenomenon is similar with that of  $\text{ZrO}_2$  when sintered at high temperature [34–36]. N.K. Simha et al. firstly constructed Bain strains for the tetragonal to monoclinic transformation of zirconia to explain the mechanism of resulting twin [37]. By introducing the twin planes, it is suspected that the strength of  $\theta$ - $\text{Al}_2\text{O}_3$  whiskers could be enhanced [38].

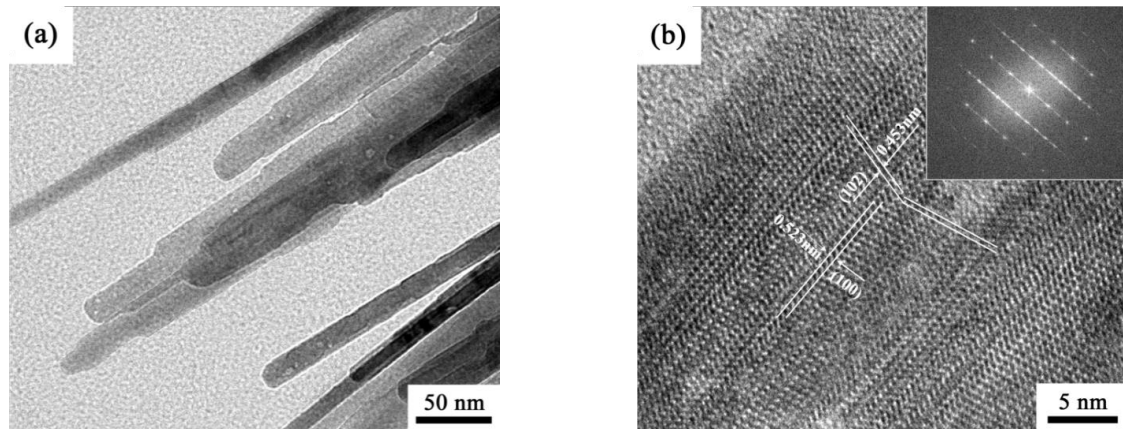


**Figure 5.** High resolution transmission electron microscope (HRTEM) images of  $\theta$ - $\text{Al}_2\text{O}_3$  whiskers prepared by the hydrothermal method with the molar ratio of  $\text{Al}^{3+}:\text{CO}(\text{NH}_2)_2$  of 1:6 followed by annealing at 1000 °C: (a) tips of whiskers and (b) twins. Inset image in Figure (b) shows the selected area electron diffraction (SAED) pattern of twins.

Figure 6 presents the adsorption-desorption curves of  $\theta$ - $\text{Al}_2\text{O}_3$  whiskers tested in nitrogen. These two curves belong to III-type with the existence of hysteresis loop which is H3-type associating with the gaps among whiskers [39]. It is calculated that the specific surface areas of  $\theta$ - $\text{Al}_2\text{O}_3$  whiskers transformed from the precursors prepared at the molar ratios of  $\text{Al}^{3+}:\text{CO}(\text{NH}_2)_2$  of 1:5 and 1:6 are high as 43.3 and 38.2  $\text{m}^2/\text{g}$ , respectively. Therefore, the as-obtained alumina whiskers are also promising to be used as the support of catalysts in the high temperature fields [40,41].

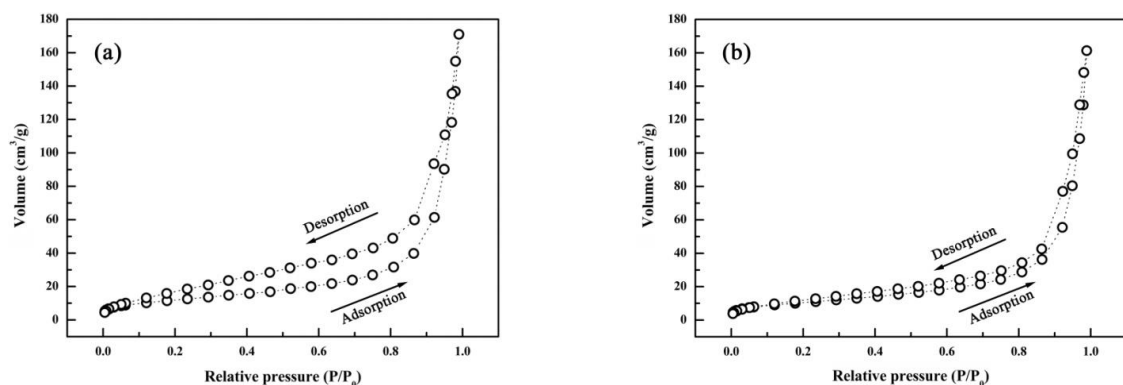


**Figure 6.** BET curves of  $\theta$ - $\text{Al}_2\text{O}_3$  whiskers fabricated by the hydrothermal method with the different molar ratio of  $\text{Al}^{3+}:\text{CO}(\text{NH}_2)_2$  of (a) 1:5 and (b) 1:6 followed by annealing at 1000 °C.

#### 4. Conclusions

This work investigated the hydrothermal synthesis of twin  $\theta$ - $\text{Al}_2\text{O}_3$  whiskers and the conclusions are summarized as follows:

- $\theta$ -Al<sub>2</sub>O<sub>3</sub> whiskers were successfully fabricated by using the hydrothermal method followed by annealing at 1000 °C in the flowing argon using Al<sub>2</sub>(SO<sub>4</sub>)<sub>3</sub>·18H<sub>2</sub>O, CO(NH<sub>2</sub>)<sub>2</sub> and PEG2000 as the initial materials.
- The optimized molar ratio of Al<sup>3+</sup>:CO(NH<sub>2</sub>)<sub>2</sub> was determined as 1:6 to obtain the homogeneous AlO(OH) precursor.
- The final morphology of  $\theta$ -Al<sub>2</sub>O<sub>3</sub> whiskers was derived from the initial microstructure of AlO(OH) precursor.
- $\theta$ -Al<sub>2</sub>O<sub>3</sub> whiskers contained twins owing to the phase transformation from tetragonal system to monoclinic system during annealing. The high specific surface area of  $\theta$ -Al<sub>2</sub>O<sub>3</sub> whiskers was measured as 38.2 m<sup>2</sup>/g.

**Author Contributions:** Conceptualization, N.L.; methodology, H.Z.; software, H.Z.; validation, X.S.; formal analysis, Q.F.; investigation, H.Z.; resources, H.Z.; data curation, S.G.; writing—original draft preparation, N.L.; writing—review and editing, X.S.; visualization, Q.F.; supervision, C.H.; project administration, C.H.; funding acquisition, C.H. All authors have read and agreed to the published version of the manuscript.

**Funding:** This research was funded by the Natural Sciences Foundation of China (52072311), Outstanding Young Scientific and Technical Talents in Sichuan Province (2019JDJQ0009), the Opening Project of State Key Laboratory of Green Building Materials and the Open Project of State Key Laboratory Cultivation Base for Nonmetal Composites and Functional Materials (20kfhg17).

**Institutional Review Board Statement:** Not applicable.

**Informed Consent Statement:** Not applicable.

**Data Availability Statement:** The data presented in this study are available on request from the corresponding author. The data are not publicly available due to all the dataset created during this research belong to the funder according to the contract.

**Conflicts of Interest:** The authors declare no conflict of interest. The funders had no role in the design of the study; in the collection, analyses, or interpretation of data; in the writing of the manuscript; or in the decision to publish the results.

## References

1. Dong, W.; Zhu, S.; Bai, T.; Luo, Y. Influence of Al<sub>2</sub>O<sub>3</sub> whisker concentration on mechanical properties of WC–Al<sub>2</sub>O<sub>3</sub> whisker composite. *Ceram. Int.* **2015**, *41*, 13685–13691. [\[CrossRef\]](#)
2. Zhu, Z.; Wei, Z.; Shen, J.; Zhu, L.; Xu, L.; Zhang, Y.; Wang, S.; Liu, T. Fabrication and catalytic growth mechanism of mullite ceramic whiskers using molybdenum oxide as catalyst. *Ceram. Int.* **2017**, *43*, 2871–2875. [\[CrossRef\]](#)
3. Lv, X.; Ye, F.; Cheng, L.; Fan, S.; Liu, Y. Fabrication of SiC whisker-reinforced SiC ceramic matrix composites based on 3D printing and chemical vapor infiltration technology. *J. Eur. Ceram. Soc.* **2019**, *39*, 3380–3386. [\[CrossRef\]](#)
4. Zou, D.; Ke, X.; Qiu, M.; Chen, X.; Fan, Y. Design and fabrication of whisker hybrid ceramic membranes with narrow pore size distribution and high permeability via co-sintering process. *Ceram. Int.* **2018**, *44*, 21159–21169. [\[CrossRef\]](#)
5. Ding, J.; Deng, C.; Yuan, W.; Zhu, H.; Li, J. The synthesis of titanium nitride whiskers on the surface of graphite by molten salt media. *Ceram. Int.* **2013**, *39*, 2995–3000. [\[CrossRef\]](#)
6. Xiong, H.; Li, Z.; Zhou, K. TiC whisker reinforced ultra-fine TiC-based cermets: Microstructure and mechanical properties. *Ceram. Int.* **2016**, *42*, 6858–6867. [\[CrossRef\]](#)
7. Chen, X.; Li, T.; Ren, Q.; Wu, X.; Dang, A.; Li, H.; Zhao, T. Fabrication and morphology control of high strength lightweight mullite whisker network. *J. Alloys Compd.* **2017**, *729*, 285–292. [\[CrossRef\]](#)
8. Zuo, F.; Meng, F.; Lin, D.-T.; Yu, J.-J.; Wang, H.-J.; Xu, S.; Guo, W.-M.; Cerecedo, C.; Valcárcel, V.; Lin, H.-T. Influence of whisker-aspect-ratio on densification, microstructure and mechanical properties of Al<sub>2</sub>O<sub>3</sub> whiskers-reinforced CeO<sub>2</sub>-stabilized ZrO<sub>2</sub> composites. *J. Eur. Ceram. Soc.* **2018**, *38*, 1796–1801. [\[CrossRef\]](#)
9. Fang, Y.; Chen, N.; Du, G.; Zhang, M.; Zhao, X.; Wu, J. Effect of Y<sub>2</sub>O<sub>3</sub>-stabilized ZrO<sub>2</sub> whiskers on the microstructure, mechanical and wear resistance properties of Al<sub>2</sub>O<sub>3</sub> based ceramic composites. *Ceram. Int.* **2019**, *45*, 16504–16511. [\[CrossRef\]](#)
10. Akatsu, T.; Takashima, H.; Shinoda, Y.; Wakai, F.; Wakayama, S. Thermal-Shock Fracture and Damage Resistance Improved by Whisker Reinforcement in Alumina Matrix Composite. *Int. J. Appl. Ceram. Technol.* **2016**, *13*, 653–661. [\[CrossRef\]](#)
11. Zhao, Z.; Johnsson, M.; Shen, Z. Microstructure and mechanical properties of titanium carbonitride whisker reinforced  $\beta$ -sialon matrix composites. *Mater. Res. Bull.* **2002**, *37*, 1175–1187. [\[CrossRef\]](#)
12. Abdullah, M.; Mehmood, M.; Ahmad, J. Single step hydrothermal synthesis of 3D urchin like structures of AACH and aluminum oxide with thin nano-spikes. *Ceram. Int.* **2012**, *38*, 3741–3745. [\[CrossRef\]](#)



13. Luo, Y.; Zheng, S.L.; Ma, S.H.; Liu, C.L.; Wang, X.H. Mullite-bonded SiC-whisker-reinforced SiC matrix composites: Preparation, characterization, and toughening mechanisms. *J. Eur. Ceram. Soc.* **2018**, *38*, 5282–5293. [\[CrossRef\]](#)
14. Zhang, Y.M.; Zeng, D.J.; Wang, B.; Yang, J.F. Effect of heating parameters on sintering behaviors and properties of mullite whisker frameworks. *Nanotechnology* **2018**, *29*, 164001. [\[CrossRef\]](#)
15. Qu, X.Y.; Wang, F.C.; Shi, C.S.; Zhao, N.Q.; Liu, E.Z.; He, C.N.; He, F. In situ synthesis of a gamma-Al<sub>2</sub>O<sub>3</sub> whisker reinforced aluminum matrix composite by cold pressing and sintering. *Mater. Sci. Eng. A* **2018**, *709*, 223–231. [\[CrossRef\]](#)
16. Tamura, Y.; Moshtaghioun, B.M.; Zapata-Solvas, E.; Gomez-Garcia, D.; Domínguez-Rodríguez, A.; Cerecedo-Fernández, C.; Valcárcel-Juárez, V. Is an alumina-whisker-reinforced alumina composite the most efficient choice for an oxidation-resistant high-temperature ceramic? *J. Eur. Ceram. Soc.* **2018**, *38*, 1812–1818. [\[CrossRef\]](#)
17. Ali, M.; Mujtaba-Ul-Hassan, S.; Ahmad, J.; Khurshid, A.; Shahzad, F.; Iqbal, Z.; Mehmood, M.; Waheed, K. Fabrication of PEGylated Porous Alumina Whiskers (PAW) for drug delivery applications. *Mater. Lett.* **2019**, *241*, 23–26. [\[CrossRef\]](#)
18. Valcárcel, V.; Souto, A.; Guitián, F. Development of single-crystal  $\alpha$ -Al<sub>2</sub>O<sub>3</sub> fibers by vapor-liquid-solid deposition (VLS) from aluminum and powdered silica. *Adv. Mater.* **1998**, *10*, 138–140. [\[CrossRef\]](#)
19. Chu, Y.; Jing, S.; Liu, D.; Ye, B. Screw dislocation assisted spontaneous growth of single-crystalline  $\alpha$ -Al<sub>2</sub>O<sub>3</sub> microrods. *Compos. Commun.* **2018**, *10*, 93–96. [\[CrossRef\]](#)
20. Ahmad, J.; Tariq, M.I.; Ahmad, R.; Ul-Hassan, S.M.; Mehmood, M.; Khan, A.F.; Waseem, S.; Mehboob, S.; Tanvir, M.T. Formation of porous  $\alpha$ -alumina from ammonium aluminum carbonate hydroxide whiskers. *Ceram. Inter.* **2019**, *45*, 4645–4652. [\[CrossRef\]](#)
21. Li, J.; Li, W.; Nai, X.; Bian, S.; Liu, X.; Wei, M. Synthesis and formation of alumina whiskers from hydrothermal solution. *J. Mater. Sci.* **2009**, *45*, 177–181. [\[CrossRef\]](#)
22. Mirzajany, R.; Alizadeh, M.; Saremi, M.; Rahimpour, M.-R. Suspension preparation of alumina whiskers for spray granulation. *Mater. Lett.* **2018**, *228*, 344–347. [\[CrossRef\]](#)
23. Zhu, Z.; Sun, H.; Liu, H.; Yang, D. PEG-directed hydrothermal synthesis of alumina nanorods with mesoporous structure via AACH nanorod precursors. *J. Mater. Sci.* **2010**, *45*, 46–50. [\[CrossRef\]](#)
24. Morinaga, K.; Torikai, T.; Nakagawa, K.; Fujino, S. Fabrication of fine  $\alpha$ -alumina powders by thermal decomposition of ammonium aluminum carbonate hydroxide (AACH). *Acta Mater.* **2000**, *48*, 4735–4741. [\[CrossRef\]](#)
25. Deng, Z.-Y.; Fukasawa, T.; Ando, M.; Zhang, G.-J.; Ohji, T. High-Surface-Area Alumina Ceramics Fabricated by the Decomposition of Al(OH)<sub>3</sub>. *J. Am. Ceram. Soc.* **2001**, *84*, 485–491. [\[CrossRef\]](#)
26. Zhang, H.; Zhu, D.; Grasso, S.; Hu, C. Tunable morphology of aluminum oxide whiskers grown by hydrothermal method. *Ceram. Int.* **2018**, *44*, 14967–14973. [\[CrossRef\]](#)
27. Bradford, S.C. On the Theory of Gels. *Biochem. J.* **1921**, *15*, 553–562.1. [\[CrossRef\]](#) [\[PubMed\]](#)
28. Digne, M.; Sautet, P.; Raybaud, P.; Toulhoat, H.; Artacho, E. Structure and Stability of Aluminum Hydroxides: A Theoretical Study. *J. Phys. Chem. B* **2002**, *106*, 5155–5162. [\[CrossRef\]](#)
29. Mirzajany, R.; Alizadeh, M.; Rahimpour, M.-R.; Saremi, M. Seed-assisted hydrothermally synthesized AACH as the alumina precursors. *Mater. Chem. Phys.* **2019**, *221*, 188–196. [\[CrossRef\]](#)
30. Łodziańska, Z.; Topsøe, N.-Y.; Nørskov, J.K. A negative surface energy for alumina. *Nat. Mater.* **2004**, *3*, 289–293. [\[CrossRef\]](#)
31. Wang, Y.G.; Bronsveld, P.M.; DeHosson, J.T.M.; Djuricic, B.; McGarry, D.; Pickering, S. Ordering of Octahedral Vacancies in Transition Aluminas. *J. Am. Ceram. Soc.* **2005**, *81*, 1655–1660. [\[CrossRef\]](#)
32. Wang, Y.; Bronsveld, P.; De Hosson, J.; Djuricic, B.; McGarry, D.; Pickering, S. Twinning in  $\theta$  Alumina Investigated with High Resolution Transmission Electron Microscopy. *J. Eur. Ceram. Soc.* **1998**, *18*, 299–304. [\[CrossRef\]](#)
33. Xue, Y.; Lin, J.; Fan, Y.; Li, J.; Elsanousi, A.; Xu, X.; Liu, N.; Huang, Y.; Hu, L.; Liu, Y.; et al. Synthesis and hydrogen absorption of high-specific-surface ultrafine theta-Al<sub>2</sub>O<sub>3</sub> nanowires. *J. Cryst. Growth* **2013**, *382*, 52–55. [\[CrossRef\]](#)
34. Shen, P.; Lee, W.H. (111)-Specific Coalescence Twinning and Martensitic Transformation of Tetragonal ZrO<sub>2</sub> Condensates. *Nano Lett.* **2001**, *1*, 707–711. [\[CrossRef\]](#)
35. Lam, K.Y.; Zhang, J.M. Transformation twinning in monoclinic zirconia particles. *Acta Met. Mater.* **1992**, *40*, 1395–1401. [\[CrossRef\]](#)
36. Lin, G.; Lei, T.; Zhou, Y. In-situ TEM observations of tetragonal to monoclinic phase transformation in ZrO<sub>2</sub>-2 mol% Y<sub>2</sub>O<sub>3</sub> ceramics. *Ceram. Int.* **1998**, *24*, 307–312. [\[CrossRef\]](#)
37. Simha, N. Twin and habit plane microstructures due to the tetragonal to monoclinic transformation of zirconia. *J. Mech. Phys. Solids* **1997**, *45*, 261–263. [\[CrossRef\]](#)
38. Guo, H.; Zhang, J.; Mao, X.; Zhang, F.; Sun, F.; Chen, F.; Wang, J.; Tian, R.; Liu, J.; Wang, S. Strengthening mechanism of twin lamellas in transparent AlON ceramics. *J. Eur. Ceram. Soc.* **2018**, *38*, 3235–3239. [\[CrossRef\]](#)
39. Zhao, B.; Song, J.; Fang, T.; Liu, P.; Jiao, Z.; Zhang, H.; Jiang, Y. Hydrothermal method to prepare porous NiO nanosheet. *Mater. Lett.* **2012**, *67*, 24–27. [\[CrossRef\]](#)
40. Wang, L.; An, L.; Zhao, J.; Shimai, S.; Mao, X.; Zhang, J.; Liu, J.; Wang, S. High-strength porous alumina ceramics prepared from stable wet foams. *J. Adv. Ceram.* **2021**, 1–8. [\[CrossRef\]](#)
41. Krivoshapkina, E.F.; Krivoshapkin, P.V.; Vedyagin, A.A. Synthesis of Al<sub>2</sub>O<sub>3</sub>-SiO<sub>2</sub>-MgO ceramics with hierarchical porous structure. *J. Adv. Ceram.* **2017**, *6*, 11–19. [\[CrossRef\]](#)